

# Deep Generative and Discriminative Digital Twin endowed with Variational Autoencoder for Unsupervised Predictive Thermal Condition Monitoring of Physical Robots in Industry 6.0 and Society 6.0

Eric Guiffo Kaigom \*

\* Department of Computer Science & Engineering,  
Frankfurt University of Applied Sciences, Frankfurt a.M., Germany  
(e-mail: kaigom@fra-uas.de).

**Abstract:** Robots are unrelentingly used to achieve operational efficiency in Industry 4.0 along with symbiotic and sustainable assistance for the work-force in Industry 5.0. As resilience, robustness, and well-being are required in anti-fragile manufacturing and human-centric societal tasks, an autonomous anticipation and adaption to thermal saturation and burns due to motors overheating become instrumental for human safety and robot availability. Robots are thereby expected to self-sustain their performance and deliver user experience, in addition to communicating their capability to other agents in advance to ensure fully automated thermally feasible tasks, and prolong their lifetime without human intervention. However, the traditional robot shutdown, when facing an imminent thermal saturation, inhibits productivity in factories and comfort in the society, while cooling strategies are hard to implement after the robot acquisition. In this work, smart digital twins endowed with generative AI, i.e., variational autoencoders, are leveraged to manage thermally anomalous and generate uncritical robot states. The notion of thermal difficulty is derived from the reconstruction error of variational autoencoders. A robot can use this score to predict, anticipate, and share the thermal feasibility of desired motion profiles to meet requirements from emerging applications in Industry 6.0 and Society 6.0.

**Keywords:** Robotics, Digital Twin, Gen AI, Unsupervised Machine Learning, Temperature Control, Extended System Intelligence, Metarobotics, Variational Autoencoder, Deep Learning

## 1. INTRODUCTION

Operating robots is often jeopardized by overheating joint motors. Thermal burns due to motor overheating is critical for the safety of humans in physical human-robot-interaction (Franka (2024), Kinova (2024)). Thermal displacements of joints compromise positioning accuracy and affect production consistency (Soga et al. (2024)). Thermal loads are continuously accentuated as robot arms maintain specific configurations (e.g., during active parking with a payload in-between manipulations) for a long period of time (see, e.g., the 2. joint in Fig. 1). Over years of operational usage, the motor temperature (e.g., around 130°C) (Song and Liang (2024), Zhu et al. (2021), Singh et al. (2021)) considerably impacts the degradation of the winding insulation. Included are the burnout of winding wire and deperting indicated in Urata et al. (2008), as well as dielectric breakdown of winding insulation due to thermal aging (Szamel and Oloo (2024)). Besides limited peak torques impairing the robot performance (Singh et al. (2021)), thermal oxidation might reduce the lifetime of electronic components (see Fig. 1), thus compromising functionalities upon which the robot performance depends.

Strategies have been developed for the passive and active thermal management of joint motors. The active approach

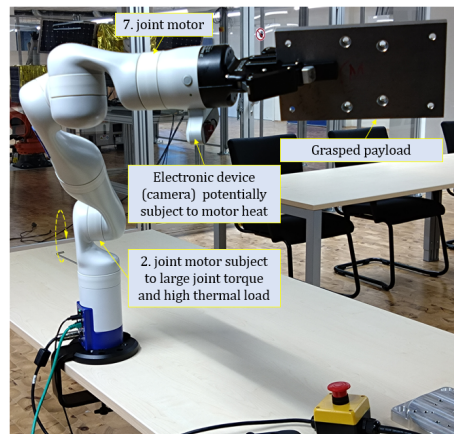


Fig. 1. Actively waiting robot under motor overheating.

includes a forced convection that typically uses e.g. electric energy to accelerate the transfer and quick accommodation of heat. By contrast, the passive strategy involves a natural conduction, convection, and radiation for heat absorption and dissipation. Passive cooling is known to be cost- and energy-effective as well as easier to implement than active cooling. However, active liquid cooling enhances the torque density (Zhu et al. (2021), Witzel et al. (2024)). Practical

Table 1. Thermal management for robots.

Passive thermal management			
Strategy	Type	Thermal Conductivity (W/mK)	Application
Heat sink (From gases to silver)	Passive	0.01 $10^3$ (Digikey (2024))	— Electronic dev.
Heat spreader (e.g., diamond)	Passive	up to $2.2 \cdot 10^3$ (coherent (2024))	InP substrate, LED, battery

insights in both thermal management techniques for robots are given in Table 1 and 2. Active immersive cooling of a BLDC motor of a legged robot has been shown to yield a thermal conductance that is 3.7 times better than in the case of a forced liquid cooling, as shown in Table 2.

Strategies mentioned thus far are relevant during the design and manufacturing of robots. They are hard to apply once the robot is being operated, as pointed out in Jorgensen et al. (2019), Kawaharazuka et al. (2020), and Singh et al. (2021). In this case, a software-based intelligent thermal control that harnesses joint states outputted by the application programming interface (API) becomes pivotal to anticipate thermal saturation. Manufacturing and even less emerging robot-driven sectors, such as healthcare/nursing and household, along with robotized space servicing (Witzel et al. (2024)), are missing such software. Deploying experts to actively manage thermal loads of robots can be prohibitive, as in space servicing (Witzel et al. (2024)). These sectors aim at using robots at a high level of availability, autonomy, and user experience.

In this paper, we propose an unsupervised framework that predicts whether the desired motion of a robot leads to overheating. The approach can generate thermally uncritical motions to anticipate a thermal saturation. To this end, a digital twin (DTw) endowed with a variational autoencoder encodes (i.e., learns) the distribution of thermally uncritical states of the robot in a lower dimensional latent space. The notion of thermal difficulty derived from the decoding (i.e. reconstruction) error is introduced to predict thermal outlier motions and offer a measure that robots can share to communicate their risks of thermal saturation for a given time horizon. Our framework helps foresee and analyze thermal outlier states in both the latent and reconstruction space.

Table 2. Thermal management of a BLDC motor of a robot (based upon Zhu et al. (2021)).

Active thermal mngt of a motor of a legged robot			
Strategy (Room temperature 26°C)	Time [s] to safety limit (125°C)	Improvement in [s]	Improvement in %
No Thermal Interface Materials (TIM) (Silicone)	3.6	-	-
TIM + Forced Air (40 mm fan)	10.69	7	197%
Forced liquid (Water)	11.59	7.9	222%
Immersion cooling (Deionized Water)	$\infty$ (i.e., Temp. $\rightarrow$ 85°C < 125°C)	max.	max.

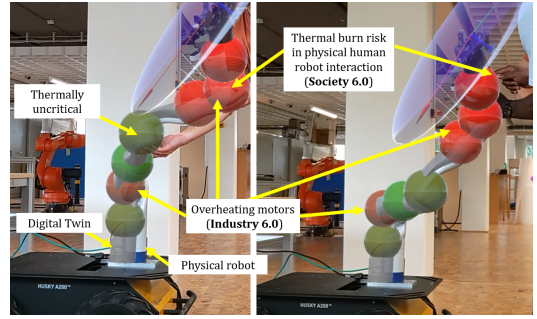


Fig. 2. Thermal monitoring (Abt et al. (2025)) and issues. Sphere = thermal motor state. Red/green = hot/cold.

It thereby offers not only visually rich and expressive but also numerical insights in the thermal behavior of joint motors for the industry and society without thermal exposition or system disassembly. The AI/ML-embedded unsupervised approach targets a sustainable citizen well-being in Society 6.0 and collective intelligence in Industry 6.0 while following the non-invasiveness goals of our overarching Metarobotics framework (Kaigom (2023)).

## 2. RELATED WORK

Efforts have been devoted to the management of the thermal behavior of robot joints. Kawaharazuka et al. (2020) leverage back-propagation to learn model parameters useful to estimate the core temperature of motors. The model can detect the augmentation of heat from the core to the housing that a motor of a musculoskeletal humanoid can face. In Singh et al. (2021), thermal control takes advantage of peak current in robot actuators. A limiter is implemented to anticipate the output temperature of the stator that closely relates to the peak temperature at which the motor operates. An intelligent temperature controller for mobile robot is proposed by Afaq et al. (2023). Fuzzy logic is designed to actively regulate temperature with minimized energy demands. Chen et al. (2024) predict the lifetime of permanent magnet synchronous motors using the insulation thermal aging. The compensation of the thermal drift error for industrial robots is addressed in Sigran et al. (2023). Difficulties to obtain temperature data of robots are pointed out as *"One of the limiting factors..."* along with *"...unfeasible system costs"* (Sigran et al. (2023)). In Demircioğlu and Yilmaz (2023), an auto-encoder (AE) predicts thermal anomalies of a DC motor through data compression and reconstruction. However, the distribution of data is omitted. The latent space is neither considered nor regularized. Discontinuities in the AE latent space are likely to impair the generation of data.

By contrast, we learn in this work the statistical distributions of observed data about the state of joints of a robot subject to a thermal process. The learned distribution is employed to detect motor overheating and create new thermally non-anomalous joint motions. We model the thermal dynamics as a generative process with stochastic hidden variables and assume Gaussian distributions. Unlike previous work, the loss function minimizes the reconstructions error and regularizes the latent space. Variational autoencoding, as originally proposed in (Kingma et al. (2017)), is the basic idea adopted in this work. Furthermore, we introduce and explore the concept of *thermal difficulty*

derived from the reconstruction error of the variational autoencoder (VAE). This score offers a measure for the degree of outlierness of planned motions w.r.t the captured data distribution omitted in previous works mentioned thus far. We evaluate its connection to hyperparameters. VAE-driven DTw of robots can employ and share this numerical score for multiple purposes. Included are the anticipation of thermal saturation and prevention of thermal burns in Industry 6.0 and Society 6.0 applications. We point out data augmentation, autonomy, and parsimony of the VAE-based DTw. We are not aware of any previous work that leverages VAE-embedded DTw to monitor and anticipate the overheating of joints of an ultra-lightweight robot (see Fig. 1), to the best of our knowledge.

### 3. METHOD

#### 3.1 General formulation

Assume the dataset  $X = \{x_1, \dots, x_n\}$  is from a random thermal process. Each observed and multichannel

$$x_i = \begin{bmatrix} q_i \\ \dot{q}_i \\ \tau_i \end{bmatrix} \in \mathbb{R}^{3 \cdot n_J} \quad (1)$$

is a robot state.  $q_i$ ,  $\dot{q}_i$ , and  $\tau_i$  are the joint positions, velocities, and total (including external) torques at timestamp  $i$ .  $n_J$  is the number of joints. For a redundant arm with  $n_J = 7$  as in Fig. 1, for example,  $x_i$  has the dimension  $d_x = 21$ .

Each  $x = x_i \in X$  is associated with an unobserved and inducing latent variable  $z = z_i \in Z = \{z_1, \dots, z_n\}$  assumed to steer the process to produce  $x$ . According to Bayes, the conditional probability distribution  $p(z|x)$  reads

$$p(z|x) = \frac{p(x|z)p(z)}{p(x)}. \quad (2)$$

The posterior distribution  $p(z|x)$  can be seen as encoding (e.g., projecting)  $x$  to yield a compressed lower dimensional  $z$ . On the other hand,  $x$  is reconstructed from the sampled  $z$  with the decoding likelihood  $p(x|z)$ , which needs to be maximized. Since the evidence given by

$$p(x) = \int p(x|z)p(z)dz, \quad (3)$$

with prior  $p(z)$ , is hard to compute for continuous  $z$ , the posterior  $p(z|x)$  is approximated by a distribution  $q_\phi(z|x)$  on the encoder side:

$$q_\phi(z|x) \approx p(z|x). \quad (4)$$

$\phi$  is a set of neural parameters to be learned. The similarity between  $p(z|x)$  and  $q_\phi(z|x)$  is enforced by minimizing the Kullback-Leibler divergence  $KL(q_\phi(z|x)||p(z|x))$  of  $q_\phi(z|x)$  from  $p(z|x)$ . To this end, the variational inference is leveraged. The minimization is equivalent to maximizing the evidence lower bound

$$\mathcal{E} = -KL(q_\phi(z|x)||p(z)) \quad (5)$$

$$+ \mathbb{E}_{q_\phi(z|x)}[\log(p_\theta(x|z))] \quad (6)$$

as lower bound of  $\log(p(x))$  since  $KL(a||b) \geq 0$  for any distribution  $a$  and  $b$ .  $\theta$  are learnable neural network weights.

#### 3.2 Specific training

In this work, the unknown latent vector has the form

$$z = z_i = \begin{bmatrix} z_{1i} \\ z_{2i} \end{bmatrix} \in \mathbb{R}^2. \quad (7)$$

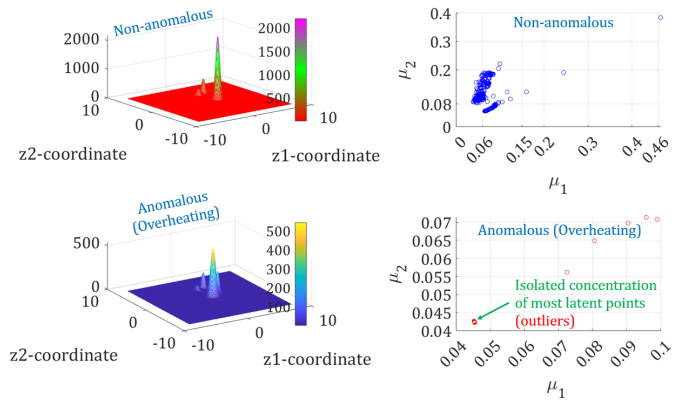


Fig. 3. L.h.s: VAE-based embedding of the data manifold ( $x_i$ ) into the lower dimensional 2D latent space visualized as superposition of learned Gaussian densities ( $\mathcal{N}(\mu_q, \Sigma_q)$ ) related to  $z_i$ . R.h.s:  $(\mu_1, \mu_2)$  associated with  $q_\phi(z_i|x_i)$  for low/high temperature data in 2D. An outlier cluster is visible in the latent space.

Observe that  $x$  in eq. 1 being compressed has more components than  $z$  in eq. 7 even for  $n_J = 1$ . Latent variables and their distributions assumed to be Gaussian can be easily visualized and further processed in the 2D latent space.  $p(z)$  is assumed to be a Gaussian distribution  $\mathcal{N}(\mu_p, \Sigma_p)$  with the mean equal to  $\mu_p = 0$  and the covariance matrix given by the identity  $\Sigma_p = \begin{bmatrix} \sigma_{p_1}^2 & 0 \\ 0 & \sigma_{p_2}^2 \end{bmatrix} = \begin{bmatrix} 1 & 0 \\ 0 & 1 \end{bmatrix}$ .  $q_\phi(z|x)$  is viewed as a Gaussian distribution (see l.h.s of Fig. 3)  $\mathcal{N}(\mu_q, \Sigma_q)$  whose parameters  $(\mu_q, \Sigma_q)$  with  $\mu_q = \begin{bmatrix} \mu_{q_1} \\ \mu_{q_2} \end{bmatrix}$  and  $\Sigma_q = \begin{bmatrix} \sigma_{q_1}^2 & 0 \\ 0 & \sigma_{q_2}^2 \end{bmatrix}$  depends upon the weights  $\phi$  of the deep neural encoding network to be trained. In this case, the regularization term in eq. 5 is

$$KL(q_\phi(z|x)||p(z)) = -\frac{\beta}{2} \sum_{j=1}^2 (1 + \log(\sigma_{q_j}^2) - \mu_{q_j}^2 - \sigma_{q_j}^2).$$

The scalar  $\beta \geq 1$  balances reconstruction and distribution capture, and fosters disentangled latents. In the second term (i.e., eq. 6), the conditional distribution is modeled as a Gaussian distribution, as in Lin et al. (2019). This term captures the expected reconstruction error evaluated as the mean squared error between the output  $x_{\text{pred.}} = \text{NN}_\theta(z)$  predicted by the neural decoding network  $\text{NN}_\theta$  (with input  $z$  and weights  $\theta$ ) and the original input  $x$  of the neural encoding network  $\text{NN}_\phi(x)$  (see Beaulac (2019)).

Encoder and decoder neural networks made up of multiple long short-term memory (LSTM) and fully connected (FC) layers are trained using stochastic gradient descent and backpropagation (Tebuch et al. (2022)). The reparameterization trick

$$z = \mu + \epsilon \odot \sigma \quad (8)$$

is employed for a stable back-propagation. Indeed, eq. 8 allows for the reduction of the variance estimate of the gradient when taking the derivative of the posterior distribution (Ghojogh et al. (2021)). In eq. 8,  $\epsilon$  is a noise variable sampled on  $\mathcal{N}(0, 1)$ .  $\odot$  is the Hadamar product used in eq. 8 to map  $\epsilon$  to  $z$  by taking advantage of  $\mu$  and  $\sigma$ .

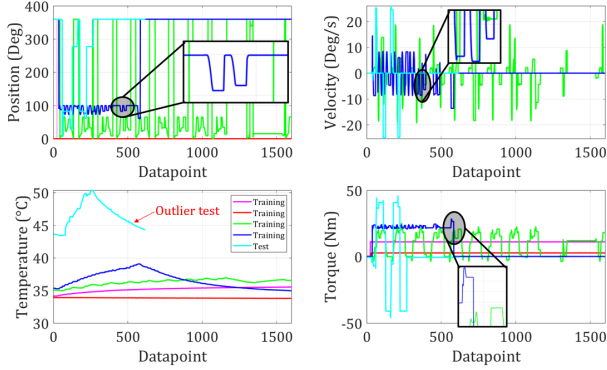


Fig. 4. Non-anomalous training ( $q(t)$ ,  $\dot{q}(t)$ ,  $\tau(t)$ ) and cyan-colored anomalous test data with large temperature.

#### 4. APPLICATIONS

Experiments have been carried out to evaluate the usefulness of using VAE-endowed DTw to monitor the thermal behavior of the second joint of the physical robot depicted in Fig. 1. Furthermore, the capability of the VAE to generate thermally non-anomalous motions has been investigated. The DTw endowed with VAE not only reflected the current state of the robot, but was also in charge of the aggregation and processing of datasets relevant for these objectives (Digital Shadow) while maintaining the traceability of the usage of the physical robot (Digital Thread). Services of the DTw leveraged the VAE to detect outlier data out of the distribution from which thermally non-anomalous training datasets are for condition monitoring.

##### 4.1 Data capture and pre-processing

$q(t)$ ,  $\dot{q}(t)$ , and  $\tau(t)$  were collected from the arm in Fig. 1 to train the VAE. Examples of acquired datasets are shown in Fig. 4. Datasets were obtained using built-in sensors. Thermally uncritical (temperature below  $40^\circ$ ) training and critical (temperature above  $40^\circ$ ) test datasets were collected (see also Table 3). Each three channel training sequence had more than  $1.5 \cdot 10^3$  datapoints (see Fig. 4). The anomalous test dataset had comparatively less datapoints than training datasets and a higher temperature range (however below the warning threshold (see Table 3)), as shown in Fig. 4. The z-score normalization was used to pre-process the unfiltered training and test datasets.

##### 4.2 Monitoring and anticipating thermal overheating

The cumulation of Gaussian probability distribution functions associated with the 2D latent vectors are depicted in

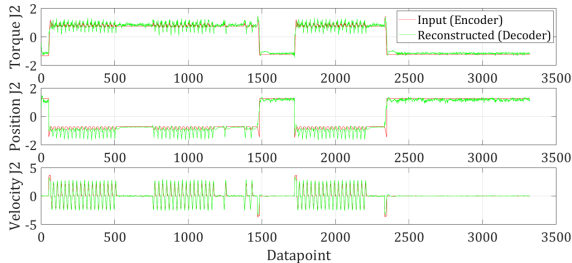


Fig. 5. Reconstruction of a non-anomalous dataset with the error smaller than in the critical case (Fig. 6).

Table 3. Data for thermal safety of the Kinova Gen 3 robot (see Kinova (2024))

Data	Lower	Upper	Warning	Error
Max. motor temperature	$0^\circ$	$80^\circ$	$60^\circ$	$75^\circ$
Max. core temperature	$0^\circ$	$100^\circ$	$80^\circ$	$90^\circ$

Fig. 3. Latent vectors related to non-anomalous training data are encoded in the upper part. Anomalous test data are projected in the lower part of Fig. 3. Clusters of mean values can be observed in the lower r.h.s. Distributions related to data in the high temperature range (see lower l.h.s of Fig. 4) are apart from remaining distributions, as indicated in the lower r.h.s of Fig. 3. Sampling from distributions in this cluster generates motions with a high overheating likelihood.

##### 4.3 Detecting thermally anomalous motion profiles

The goal was to detect joint states with high overheating potential by assessing issues encountered by the VAE to reconstruct original input data. Anomalous datasets are characterized by a cumulative reconstruction error between encoded and decoded data above a given threshold. The VAE was first trained using sensed data without any labeling. Hence, out-of-distribution datasets were considered to alleviate over-fitting. Then, the trained VAE was excited with anomalous test datasets from the lower l.h.s of Fig. 4. Fig. 6 reveals that the VAE-DTw hardly reconstructs original anomalous data in contrast to the non-anomalous case provided by Fig. 5.

##### 4.4 Generating thermally non-anomalous motions

Latent vectors were sampled according eq. 8 during the decoding step.  $z$  was obtained from  $\epsilon$  as stochastic input as well as means and standard deviations of approximated distributions related to thermally non-anomalous data. It was observed that generated states are close to non-anomalous data for small perturbation in the latent space. Two reconstructions triggered by different values of  $\epsilon$  are shown Fig. 9. Created position profiles are normalized and thermally non-anomalous for the targeted joint motor.

## 5. DISCUSSION

Technological, societal, and industrial implications of the framework are discussed. Training insights are provided.

##### 5.1 Implications for the Digital Twin Concept

A DTw aware of  $p_\theta(x|z)$  and  $q_\phi(z|x)$  is advantageous for at least two reasons. First, the DTw can harness the encoder

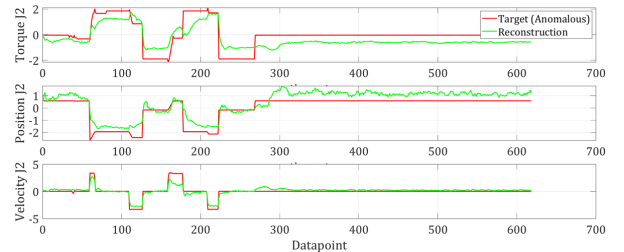


Fig. 6. Reconstruction of a high-temperature dataset. The error is larger than in the non-critical case in Fig. 5.

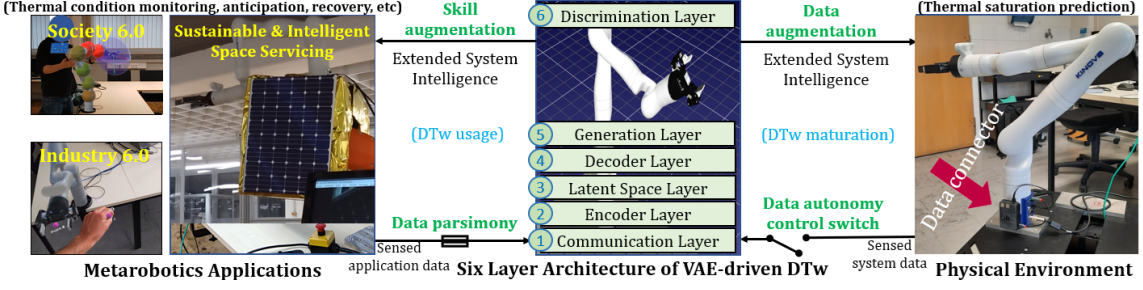


Fig. 7. Development, maturation, and usage of VAE-based DTw for thermal monitoring, analysis, and control in robotized applications. Data parsimony and autonomy are key features of the underlying extended system intelligence.

driven by  $q_\phi(z|x)$  to autonomously infer knowledge from datasets. Included are dimension reduction and clustering for data analysis and anomaly detection. Secondly, the DTw can use noise (i.e.,  $\epsilon$ ) to yield  $z$  as input of the decoder driven by  $p_\theta(x|z)$  to create new and similar (in terms of distribution) or augmented data for different purposes. Training machine learning models that support services of the DTw on-the-fly is an example. After training, running the VAE-based DTw no longer necessitates a tightly coupled data flow from the physical hardware to the DTw. In fact, the DTw can generate its own datasets with relevance. This leads to a data parsimony and even autonomy of the DTw once it has built its stochastic generative model, as highlighted in Fig. 7. In this case, the VAE model can serve as a basis for deep transfer learning to downstream applications. The idea is to employ a VAE-driven sustainable DTw to yield a regularized and shared latent feature space that fosters transferability and preserve discriminability across applications (see, e.g., Ye et al. (2022)) while requiring less data (see Fig. 7).

## 5.2 Collective intelligence implications for Industry 6.0

A robot endowed with a VAE-based DTw for thermal management can predict its thermal difficulty

$$d = \sum_{k=1}^{n_J} d_k \quad (9)$$

that arises from a planned motion. Herein,

$$d_k = 1 - e^{-\frac{1}{n} \int_{t_l}^{t_h} |e_{r_k}(t)| dt} \quad (10)$$

is the thermal difficulty of the  $k$ -th motor for the time horizon  $t \in [t_l, t_h]$ .  $|e_{r_k}(t)|$  is the absolute value of the current reconstruction error related to the targeted profile  $x(t)$  of the  $k$ -th joint state cumulatively for all channels (i.e., joint positions, velocities, and torques). According

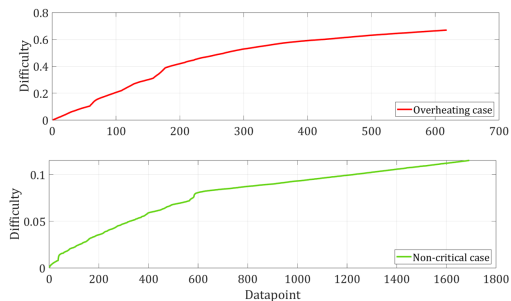


Fig. 8. Thermal difficulty for critical/non-critical data.

eq. 10 and Fig 8,  $d_k \rightarrow 1$  for anomalous  $x(t)$ . For thermally non-anomalous  $x(t)$ ,  $d_k \rightarrow 0$ . Robots can mutually exchange their  $d$  to be aware in advance of the respective capability to contribute to common goals without getting stuck in a thermal saturation. Robots informed by their VAE-embedded DTw that provide  $d$  can thermally anticipate their self-orchestration without human intervention, as expected in Industry 6.0 ((Carayannis et al. (2024)). Although  $|e_{r_k}(t)|$  indicates outliers, it was observed while training VAE-models that it does not necessarily decrease as the number of epochs increases (see table 4). This is also due to the random initialization of neural weights.

Table 4. Normalized reconstruction error  $r_e$  as a function of the number of epochs  $n_e$ .

Channel	$n_e = 20$	$n_e = 40$	$n_e = 60$	$n_e = 120$	$n_e = 240$
Torque	0.1740	0.1163	0.1781	0.0832	0.2079
Position	0.4132	0.3576	0.1621	0.1542	0.0885
Velocity	0.7043	0.4967	0.5992	0.4395	0.3185

## 5.3 Self-achievement implications for Society 6.0

Humans use physical contact interaction forces to communicate and guide compliant collaborative robots. The desired symbiosis between humans and robots is conditioned by an engaging user perception of robots for self-fulfillment. To avoid threatening thermal burn hazards (see EN ISO 13732-1:2006), employ robots to augment humans, and support the comfortable autonomy in societal tasks (e.g., household, healthcare, etc), robot manufacturers automatically shut down the robot to meet their social responsibility in terms of safety (Kinova (2024), Franka (2024)). Beyond shutdowns, a VAE-driven DTw uses the predictive thermal difficulty presented thus far to convey a spatial insight into the missing thermal awareness of robot motors (see, e.g., upper l.h.s of Fig. 7). In combination with augmented reality, the Gen AI-embedded DTw allows the robot to predict the overheating behavior of its motors using spheres with a color gradient that maximizes the thermal salience in visualized postures accessible to almost everyone and everywhere. The omnipresent and embodied AI helps anticipate thermal burns and recover from a thermal saturation through manual posture optimization and

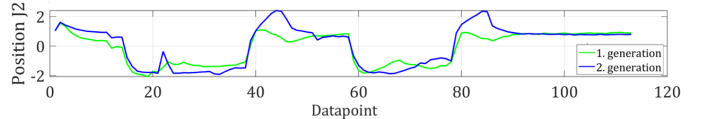


Fig. 9. Non-critical motions created by a VAE-based DTw.

avoid downtime. This reconfiguration can also be achieved using the generative skills of the VAE-driven DTw. In fact, Fig. 9 shows two uncritical motions created using different  $\epsilon$  in eq. 8 while remaining on the learned data distribution.

## 6. CONCLUSION

This work captures the distribution of joint data for the discriminative and generative thermal management of robot actuators. It introduces the thermal difficulty score as a means to share the thermal condition of robot joints for a desired motion. The score depends upon the reconstruction error of the variational autoencoder with which the digital twin of the robot is equipped to detect thermally anomalous and generate thermally uncritical state of joints. The underlying two dimensional latent space is used to transform captured distributions associated with non-anomalous joint states into opportunities for robotized application in the society 6.0 and industry 6.0 realm.

*Acknowledgments:* We would like to thank Mr. T. K. La for data collection.

## REFERENCES

Abt, P., Harmann, R., and Kaigom, E.G. (2025). Manipulability optimization and thermal control of industrial robots in real-time using digital twins, augmented reality, and opc ua. *IEEE/SICE Int. S. on Sys. Int. 2025*.

Afaq, M., Jebelli, A., and Ahmad, R. (2023). An intelligent thermal management fuzzy logic control system design and analysis using ansys fluent for a mobile robotic platform in extreme weather applications. *Journal of Intelligent & Robotic Systems*, 107(1), 11.

Beaulac, C. (2019). Variational autoencoders: Theory, implementation and unanswered questions.

Carayannis, E.G., Posselt, T., and Preissler, S. (2024). Toward industry 6.0 and society 6.0: The quintuple innovation helix with embedded ai modalities as enabler of public interest technologies strategic technology management and road-mapping. *IEEE Transactions on Engineering Management*.

Chen, M., Zhang, B., Li, H., Gao, X., Wang, J., and Zhang, J. (2024). Lifetime prediction of permanent magnet synchronous motor in selective compliance assembly robot arm considering insulation thermal aging. *Sensors*, 24(12), 3747.

coherent (2024). Dimond heat spreader. <https://www.coherent.com/news/glossary/diamond-heat-spreader>. [accessed 31-Dec-2024].

Demircioğlu, E.H. and Yilmaz, E. (2023). A method based on an autoencoder for anomaly detection in dc motor body temperature. *Applied Sciences*, 13(15), 8701.

Digikey (2024). Heat Sink Design Facts & Guidelines for Thermal Analysis. <https://www.digikey.com/Site/Global/Layouts/DownloadPdf.ashx?pdfUrl=F51974C9A6D544F1A7D8F119514B67FF>. [acc. 31.12.24].

Franka (2024). FRANKA RESEARCH 3, Product Manual. [https://download.franka.de/documents/Product%20Manual%20Franka%20Research%203\\_R02210\\_1.0\\_EN.pdf](https://download.franka.de/documents/Product%20Manual%20Franka%20Research%203_R02210_1.0_EN.pdf). [Online; accessed 31-Dec-2024].

Ghojogh, B., Ghodsi, A., Karray, F., and Crowley, M. (2021). Factor analysis, probabilistic principal component analysis, variational inference, and variational autoencoder. *Tutorial and Survey*.

Jorgensen, S.J., Holley, J., Mathis, F., Mehling, J.S., and Sentis, L. (2019). Thermal recovery of multi-limbed robots with electric actuators. *IEEE Robotics and Automation Letters*, 4(2), 1077–1084.

Kaigom, E.G. (2023). Metarobotics for industry and society: Vision, technologies, and opportunities. *IEEE Transactions on Industrial Informatics*.

Kawaharazuka, K., Hiraoka, N., Tsuzuki, K., Onitsuka, M., Asano, Y., Okada, K., Kawasaki, K., and Inaba, M. (2020). Estimation and control of motor core temperature with online learning of thermal model parameters: Application to musculoskeletal humanoids. *IEEE Robotics and Automation Letters*, 5(3), 4273–4280.

Kingma, D.P. et al. (2017). *Variational inference & deep learning: A new synthesis (Ph.D. Thesis)*.

Kinova (2024). Kinova Gen 3, Product Manual. <https://www.kinovarobotics.com/uploads/User-Guide-Gen3-R07.pdf>. [accessed 31.12.2024].

Lin, S., Roberts, S., Trigoni, N., and Clark, R. (2019). Balancing reconstruction quality and regularisation in elbo for vaes. *arXiv preprint arXiv:1909.03765*.

Sigron, P., Aschwanden, I., and Bambach, M. (2023). Compensation of geometric, backlash, and thermal drift errors using a universal industrial robot model. *IEEE Transactions on Automation Science and Engineering*.

Singh, A., Kashiri, N., and Tsagarakis, N. (2021). Thermal control for peak operation of electric robotic actuators. In *2021 20th International Conference on Advanced Robotics (ICAR)*, 763–770. IEEE.

Soga, T., Hanai, H., Hirogaki, T., and Aoyama, E. (2024). Skillful operation of working plate for grasp less ball handling with an industrial dual-arm robot considering temperature of joint motors. *International Journal of Modeling and Optimization*, 14(4).

Song, Z. and Liang, Y. (2024). Overview of high overload motors. *IEEE Transactions on Industry Applications*.

Szamel, L. and Oloo, J. (2024). Monitoring of stator winding insulation degradation through estimation of stator winding temperature and leakage current. *Machines*.

Terbuch, A., O’Leary, P., and Auer, P. (2022). Hybrid machine learning for anomaly detection in industrial time-series measurement data. In *2022 IEEE International Instrumentation and Measurement Technology Conference (I2MTC) (I2MTC 2022)*. Ottawa, Canada. URL [https://github.com/anikaTerbuch/Matlab-AE\\_MVTS](https://github.com/anikaTerbuch/Matlab-AE_MVTS).

Urata, J., Hirose, T., Namiki, Y., Nakanishi, Y., Mizuuchi, I., and Inaba, M. (2008). Thermal control of electrical motors for high-power humanoid robots. In *2008 ieee/rsj international conference on intelligent robots and systems*, 2047–2052. IEEE.

Witzel, T., Smolka, A., Plebisch, A., and Guenther, M. (2024). Analysis of liquid-cooled brushless motor actuators for space robotics. Technical report, Copernicus Meetings. URL <https://meetingorganizer.copernicus.org/EPSC2024/EPSC2024-784.html>.

Ye, M., Chen, J., Xiong, F., and Qian, Y. (2022). Learning a deep structural subspace across hyperspectral scenes with cross-domain vae. *IEEE Transactions on Geoscience and Remote Sensing*, 60, 1–13.

Zhu, T., Ahn, M.S., and Hong, D. (2021). Design and experimental study of bldc motor immersion cooling for legged robots. In *2021 Intl. Conf. on Adv. Rob. (ICAR)*.